Image fusion incorporating parameter estimation optimized Gaussian mixture model and fuzzy weighted evaluation system: a case study in time-series plantar pressure dataset

Dan Wang[1,2], Zairan Li[1, 2], Luying Cao[3], Valentina E Balas[4],Nilanjan Dey[5], Amira S. Ashour[6], Pamela McCauley[7], Sifaki-Pistolla Dimitra[8],and Fuqian Shi[3,*], *IEEE Senior Member*

***Abstract*—The key issue in image fusion is the process of defining evaluation indices for the output image and for multi-scale image dataset. The current study attempted to develop a fusion model for plantar pressure distribution images, which is expected to contribute to feature points construction based on shoe-last surface generation and modification. Firstly, the time series plantar pressure distribution image was preprocessed including back removing, Laplacian of Gaussian (LoG) filter. Then, discrete wavelet transform (DWT) and a multi-scale pixel conversion fusion operating using a parameterestimation optimized Gaussian mixture model (PEO-GMM) was performed. The output image was used in a fuzzy weighted evaluation system (FWES), that included the following evaluation indices: mean (M), standard deviation (SD), entropy (E), average gradient (AG) and spatial frequency (SF); the difference with the reference image including the root mean square error (RMSE), signal to noise ratio (SNR) and the peak SNR; and the difference with source image including the cross entropy (CE), joint entropy (JE), mutual information (MI), deviation index (DI), correlation coefficient (CC), and the degree of distortion (DD). These parameters were used to evaluate the results of the comprehensive evaluation value for the synthesized image. The image reflected the fusion of plantar pressure distribution using the proposed method compared to other fusion methods such as up-down, mean-mean and max-min fusion. The experimental results showed that the proposed LoG filtering with PEO-GMM fusion operator outperformed other methods.**

***Index Terms*—multi-scale fusion, plantar pressure imaging, parameter estimation optimized Gaussian mixture model, fuzzy weighted evaluation system**

Submitted Date: July 4, 2016. This work was supported in part by Zhejiang Provincial Natural Science Foundation (LY17F030014).

Dan Wang and Zairan Li are with 1.Tianjin Key Laboratory of Process Measurement and Control, School of Electrical Engineering and Automation, TianjinUniversity, 300072, P.R. China, and 2. WenzhouVocational & TechnicalCollege, Wenzhou, 325035, P.R. China (wangdan18111@126.com and lzr@wzvtc.cn).

Luying Cao is with 3. College of Information & Engineering, WenzhouMedicalUniversity, Wenzhou, 325035, PR China (email: 1294502807@qq.com).

Valentina E Balas is with4. Department of Automation and Applied Informatics, Aurel Vlaicu University of Arad, Arad, 310130, Romania (email: balas@drbalas.ro).

Nilanjan Dey is with 5. Dept. of IT, Techno India College of Technology, West Bengal, 740000, India (email: neelanjan.dey@gmail.com).

Amira S. Ashour is with 6. Department of Electronics and Electrical Communications Engineering, Faculty of Engineering, Tanta University, Egypt (email: amirasashour@yahoo.com).

Pamela McCauley is with 7. Department of Industrial Engineering and Management Systems, University of Central Florida, Orlando, FL, 32825, USA (email: pamela.mccauley@ucf.edu).

Dr. Sifaki-Pistolla Dimitra is an epidemiology researcher and GIS expert in the Clinic of Social and Family Medicine, Faculty of Medicine, University of Crete. (spdimi11@gmail.com)

Fuqian Shi is with College of Information & Engineering, Wenzhou Medical University, Wenzhou, 325035, PR China as corresponding author (email: sfq@wmu.edu.cn).

I. INTRODUCTION

HUMAN obtain diverse information from the external environment, while they manage to identify or perceive objects and environmental conditions due to their senses.This information may be uncertain, subjective, apprehensive, or fallacious. Different characteristics measurement, acquisition and refining of the physical phenomena may occur across the different spatial and temporal units [1] [2]. During the last few decades, the information technologies have been extensively studying these phenomena. It has been obvious that there is a rapid innovative advancement of image fusion emphasizing on the urgency for new image processing procedures to fuse on images from different scale for further analysis. Image fusion carries the salient features of multiple fused images to produce a single output image through the combination of multiple images. Predominantly, fusion methods are relevant when the imaging conditions and capture devices have limitations for capturing complete details in a single image [3].

The image fusion normally refers to merging of information from varying sources and to obtaining data from different time and space points; it is an integrated process to capture the real environment more accurately and reliably. Information fusion uses data mining technology and integration of data from unstructured or semi-structured resources [4]. Fusion provides reasonable control to the plurality of information sources in space or time according to a set of guidelines. This allows a consistent interpretation of the measured object, thus the information system can obtain superior performance compared to the one of a subset of the composition components [5]. Multi-scale, multi-resolution and multi-focus image fusion has already been developed based on the basic image fusion technology combined with artificial intelligence and

mathematical tools application such as artificial immune algorithm (AIA) [6] and Curvelet transform [7]. Fast mutual modulation fusion for multi-sensor images [8], evidence-based fusion [9] and covariance intersection (CI) fusion [10] have also been developed to improve the obtained image. He *et al*. [11] has introduced a novel infrared-to-visible image fusion algorithm for enhancing contrast and visibility. Otherwise, non-subsampled shearlet transform (NSST) and multi-scale top-hat transform (MTHT) [12], localization methods [13], contourlet transform [14] have been discussed in the literature for improving the output images. There is a complexity to automatically fuse the images accurately due to the fact that the image acquisition mode, resolution, quality, space and time characteristics are different in various imaging systems due to the dissimilar imaging principles. From those fused methods, the Guassian Mixed Model (GMM) based algorithms for image fusion has proved to be feasible and effective according to previous studies. Normally, Gaussian mixture modeling uses a fixed Gaussian distribution function, where each Gaussian model corresponds to the image state [15]. Ji *et al*. [16] deployed a magnetic resonance (MR) image segmentation of brain using adaptive scale fuzzy local GMM (Gaussian mixture model) and fuzzy clustering integration of the weighted GMM. Other artificial intelligence and data mining technology were applied in multi-scale image fusion issue. Jiang *et al.* developed a self-Generating Neural Network (SGNN) and fuzzy logic combining with wavelet multi-resolution for MR segmentation in preprocess stage of the fusion [17][18]. Li *et al*. addressed an information granulation-based fuzzy radial basis function neural networks (IG-FRBFNN) to obtain weight of each source image dynamically for improving the resulting image [19]. Banerjee *et al*. [20] applied fuzzy c-means approach for tissue classification.

Similarly to the multi-focus and multi-resolution image fusion, multi-scale fusion has special features to be considered. These fusion techniques include pyramid transform, wavelet transform, pixel selection, region-based selection, and window selection [21] [22] [23]. Recently, the wavelet multi-resolution decomposition was used for pixel-level image fusion, such as Balasubramaniam intuitionistic fuzzy sets and discrete wavelet transform for multi-resolution fusion [24]. Image fusion technology remains a new area of research for understanding and comprehensive use of the information sets. Typically, there are some common fusion methods for different types of images, including the absolute value of the greater coefficient, the weighted average method and the dual threshold [25].

Furthermore, research on plantar pressure distribution has been applied in many fieldsand has attracted a lot of scholars' attention, such as footwear, surgical medical rehabilitation and sports. Comprehensive studies on plantar pressure distribution may provide an answer on how to alleviate the pressure on patients' feet. Plantar pressure distribution combining with shoe-last design can effectively reduce the occurrence of foot disease and improve the comfort of shoes; it has great practical significance towards improving patients' quality of life. Keijsers *et al*. introduced a higher efficiency to get biomechanical behavior of interest based on time series dataset through reducing parameters of plantar pressure [26] [27]. Motha *et al*. proposed a printed pressure sensor embedded rubber insole for measurement and analysis of plantar pressure which was detected with locally embedded sensors to register various foot postures [28]. The plantar pressure research on diabetes also drew significant attraction [29] [30]. Several artificial intelligence technologies, such as data mining and marching learning were applied in feature extraction of plantar pressure dataset.

The current study on fusion algorithm aims to develop the parameter optimized Gaussian mixed model to overcome its current shortcomings. After fused operation using multi-scale fusion, a new evaluation for this multi-scale fused image was developed. In particular, a weighted fuzzy indices system for all features of the output image was developed and tested, including: cross entropy, joint entropy, mutual information, mean, standard deviation, root mean square error (RMSE), deviation index, correlation coefficient, distortion index, signal to noise ratio (SNR), peak signal to noise ratio (PSNR), average gradientand the spatial frequency. Moreover, an evaluation (FWES, fuzzy weighted evaluation system) was conducted using combined structural similarity and subjective evaluation. The knowledge system is a fuzzy expert system, which is presented by fuzzy rules like "IF-THEN" and this can also be represented as fuzzy, vague or imprecise prosperities. Point-valued fuzzy sets and weight assignment were informed as fuzzy weighted evaluation. Advantages of this proposed model are related to the discrete fuzzy set and the avoidance of complex fuzzy relational matrix. In addition, it is a multi-criteria decision making problem that includes both qualitative and quantitative criteria. Zavadskas [31] developed a weighted aggregated sum method combined with intuitionistic fuzzy numbers for product evaluation. Miguel proposed a weighted Fuzzy Inference System for air quality evaluation [32]. A fuzzy weighted average approach was also introduced for product development projects by Relich [33]. The main contribution of this study includes: i) developing an improved PEO-GMM model for image fusion and ii) developing an index system and using a fuzzy weighted evaluation system for the result image.

The organization of the remaining sections is as follows. Section II introduces the framework of this work; Section III introduces the proposed methods and algorithms for preprocessing, PEO- GMM fusion model, and fuzzy evaluation –FWES for the resultant image. Section IV represents the case study of plantar pressure image set features extraction using the proposed methodology. Finally, in Sect. V, conclusion and ideas for future work are depicted.

II. FRAMEWORKS

The current study framework involved three phases; the preprocessing, data manipulation and result evaluation. The GMM parameters were adjusted based on fusion operation to provide superior resultant images through weighted fuzzy evaluation system as shown in Figure 1. Figure 1 demonstrates the proposed overall framework for the time-series based plantar pressure imaging data fusion incorporating an improved Gaussian mixture operator. It also depicts the time-series based plantar pressure image dataset that was the input of the proposed system (the time-series based plantar pressure image dataset). Initially, a pre-processing for the image set was performed using the Discrete Wavelet Transform (DWT) and

This article has been accepted for publication in a future issue of this journal, but has not been fully edited. Content may change prior to final publication. Citation information: DOI 10.1109/JSEN.2016.2641501, IEEE Sensors Journal

pixel conversation for the multi scaled dataset. In addition, the region selection for a certain area in the foot image relative to the interest point was determined; automatically extracted by software Footscan 7. The innovative idea of the current study for the fusion algorithm is called PEO-GMM (parameter estimation optimized Gaussian mixed model). Thus, finally the result image was evaluated in comparing analyses using a fuzzy set-FWES (fuzzy weighted evaluation system). The FWES involved three parts, namely i) full information evaluation by measuring the mean, standard deviation, average gradient and spatial frequency, ii) evaluate the difference with the reference image through calculating the RMSE, SNR, PSNR, iii) evaluate the difference with the source image by measuring the cross entropy (CE), joint entropy (JE), mutual information (MI), deviation index (DI), correlation coefficient (CC), and the degree of distortion (DD).

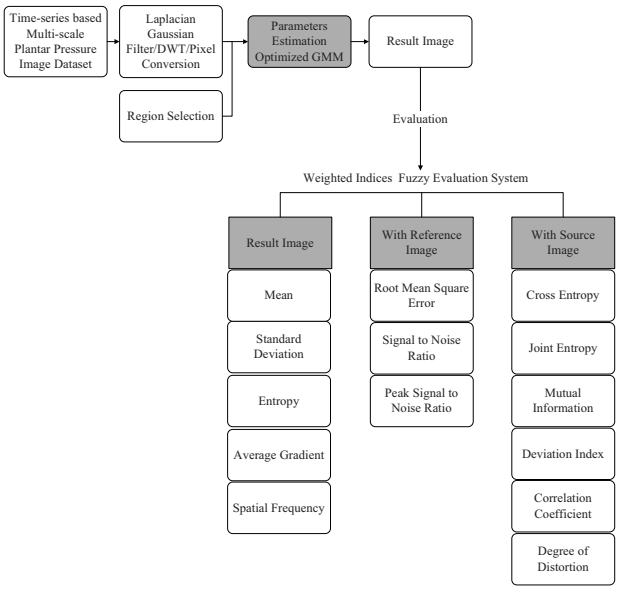

Fig. 1. The framework of time-series based plantar pressure imaging data fusion using improved GMM

III. Methods and Algorithms

The GMM parameters were adjusted based on fusion operation to provide superior resultant images through weighted fuzzy evaluation system. The proposed system was applied on a time-series based plantar pressure image datasetwhich was obtained from Footscan 7.0 system of Rsscan International. Section (IV) introduces the detailed information about experiments for obtaining dataset which was used to evaluate the proposed system performance.

A. The Image Dataset Preprocessing

1) Laplace Gaussian transform

Typically, the Laplace operator is widely used for edge detection process [34] [35] [36]. It is based on the image of the two orders reciprocal zero crossing point to determine the edges in the image using the following formula:

$$\nabla^2 f(x,y) = \frac{\partial^2 f(x,y)}{\partial x^2} + \frac{\partial^2 f(x,y)}{\partial y^2} \tag{1}$$

Since the Laplace operator realized the edge detection process through the differential operation of the image, it was sensitive to the discrete points and the noise. In order to improve the Laplace operator's robustness against noise and discrete points, the Gaussian convolution noise reduction filtering process was applied initially to all images before the Laplace operator for edge detection. This led to the Laplacian of Gaussian operator (LoG) approach. Gaussian convolution expression of the Gauss function was as follows:

$$G_\sigma(x,y) = \frac{1}{\sqrt{2\pi\sigma^2}} e^{(-\frac{x^2+y^2}{2\sigma^2})} \tag{2}$$

, where, σ was the standard deviation, (x, y) were the coordinates of the f point in image.

The expression of the original image and Gauss convolution was as follows:

$$\Delta[G_\sigma(x,y) * f(x,y)] = [\Delta G_\sigma(x,y)] * f(x,y) = LoG * f(x,y) \tag{3}$$

, where $f(x,y)$ was the original image under concern, and LoG is the Laplacian of Gaussian operator.

For the LoG, the partial derivative of the $\Delta G_\sigma(x,y)$, followed by the Gaussian convolution, was given by:

$$\begin{aligned}\frac{\partial}{\partial x}\Delta G_\sigma(x,y) &= \frac{1}{\sqrt{2\pi\sigma^2}}\frac{\partial}{\partial x}e^{-\frac{x^2+y^2}{2\sigma^2}} = \frac{1}{\sqrt{2\pi\sigma^2}}e^{-\frac{x^2+y^2}{2\sigma^2}}(-\frac{x}{\sigma^2}) \\ &= -\frac{1}{\sqrt{2\pi}\sigma^3}xe^{-\frac{x^2+y^2}{2\sigma^2}}\end{aligned} \tag{4}$$

$$\begin{aligned}\frac{\partial^2}{\partial x^2}\Delta G_\sigma(x,y) &= \frac{\partial}{\partial x}(-\frac{1}{\sqrt{2\pi}\sigma^3}xe^{-\frac{x^2+y^2}{2\sigma^2}}) \\ &= -\frac{1}{\sqrt{2\pi}\sigma^3}(e^{-\frac{x^2+y^2}{2\sigma^2}} + xe^{-\frac{x^2+y^2}{2\sigma^2}}(-\frac{x}{\sigma^2})) \\ &= \frac{x^2-\frac{1}{\sigma^2}}{\sqrt{2\pi}\sigma^3}e^{-\frac{x^2+y^2}{2\sigma^2}}\end{aligned} \tag{5}$$

The same was performed with respect to y as follows:

$$\frac{\partial^2}{\partial y^2}\Delta G_\sigma(x,y) = \frac{y^2-\frac{1}{\sigma^2}}{\sqrt{2\pi}\sigma^3}e^{-\frac{x^2+y^2}{2\sigma^2}} \tag{6}$$

Thus, the LoG expression was given by:

$$LoG \triangleq \Delta G_\sigma(x,y) = \frac{x^2+y^2-\frac{2}{\sigma^2}}{\sqrt{2\pi}\sigma^3}e^{-\frac{x^2+y^2}{2\sigma^2}} \tag{7}$$

Consequently, the Laplace Gaussian edge detection algorithm steps were the following:

Step 1. Perform the LoG convolution of the original image.

Step 2. Detect the zero crossing point (crossings zero) from negative to positive or from positive to negative.

Step 3. Threshold the zero crossing values.

2) Discrete Wavelet Transform

All images were pre-processed using the DWT before the fusion procedure. Discrete wavelet Transform means discrete input and discrete output. There was no simple formula to describe the principle stages for the definition with calculation [37].

Let $d[n]$ be the discrete input signals and divided as K segments, n is the length of the signal. Assume $g[n]$ to be the low pass filter, which filtered high frequency part, $h[n]$ be the high pass filter which filtered the low frequency part; $\downarrow Q$ be the down-sampling filter. Thus, if $d[n]$ is the input, then $w[n]=d[Qn]$ is the output, let $Q=2$ for image fusion in this paper.

Stage 1: $d_{1,L}[n]=\sum_{k=0}^{K-1} d[2n-k]g[k]$,

$$d_{1,H}[n]=\sum_{k=0}^{K-1} d[2n-k]h[k] \tag{8}$$

Stage 2: $d_{2,L}[n]=\sum_{k=0}^{K-1} d_{1,L}[2n-k]g[k]$,

$$d_{2,H}[n]=\sum_{k=0}^{K-1} d_{1,H}[2n-k]h[k] \tag{9}$$

Stage 3: $d_{\alpha,L}[n]=\sum_{k=0}^{K-1} d_{\alpha-1,L}[2n-k]g[k]$,

$$d_{\alpha,H}[n]=\sum_{k=0}^{K-1} d_{\alpha-1,H}[2n-k]h[k] \tag{10}$$

Note that the length of signal in the stage α is $\frac{N}{2^{\alpha}}$, now if the input signal is $s[m,n]$, then we make low pass and high pass filter on it, thus the following expression is obtained:,

$$v_{1,L}[m,n]=\sum_{k=0}^{K-1} s[m,2n-k]g[k] \tag{11}$$

$$v_{1,H}[m,n]=\sum_{k=0}^{K-1} s[m,2n-k]h[k] \tag{12}$$

In addition, the low pass/high pass operator on $v_{1,L}[m,n]$, $v_{1,H}[m,n]$ as follows:

$$v_{1,LL}[m,n]=\sum_{k=0}^{K-1} v_{1,L}[2m-k,n]g[k] \tag{13}$$

$$v_{1,HL}[m,n]=\sum_{k=0}^{K-1} v_{1,L}[2m-k,n]h[k] \tag{14}$$

$$v_{1,LH}[m,n]=\sum_{k=0}^{K-1} v_{1,H}[2m-k,n]g[k] \tag{15}$$

$$v_{1,HH}[m,n]=\sum_{k=0}^{K-1} v_{1,H}[2m-k,n]h[k] \tag{16}$$

Consequently, this DWT operator was used in the proposed system for fusion. After the fusion process, the inverse process of DWT (iDWT) in the composition image was performed. Contrary to decomposition, the reconstruction process was comprised of up-sampling and filtering. The Haar wavelet was a sequence of rescaled "square-shaped" functions which together form a wavelet family or basis to provide an orthonormal system for the space of square-integrable functions on the unit interval $[0,1]$. Haar transform for the scale normalization was given by:

$$\mathbf{H}_2=\frac{1}{\sqrt{2}}\begin{pmatrix}1 & 1\\ 1 & -1\end{pmatrix} \tag{17}$$

B. Gaussian Mixed Model

The Gaussian distribution was a continuous probability distribution with a bell-shaped probability density function (PDF) in one-dimensional space [38] [39] [40] given by:

$$f(x,\mu,\sigma^2)=\frac{1}{\sqrt{2\pi}\sigma}e^{-\frac{1}{2}(\frac{x-\mu}{\sigma})^2} \tag{18}$$

The parameter μ is the mean or expectation and σ^2 was the variance. The Single Gaussian Model (SGM) was applied to induct the density function of the proposed information structure *I* was defined in the current work as:

$$\delta(X,\mu,\Delta)=\frac{1}{\sqrt{(2\pi)^3\left|\Delta\right|}}e^{-\frac{1}{2}(X-\mu)^T\Delta^{-1}(X-\mu)} \tag{19}$$

, where, X was a vector in n-dimensional space, Δ was the covariance matrix, and μ was the mean value of the density function. The density function's properties were determined by (Δ,μ), which was a parameter estimation problem. For any point $P_i\in R^n$, its probability density function was $\delta(P_i,\mu,\Delta)$. For any image set I_k, each P_i in I_k was considered to be an independent event, then the PDF of I_k was:

$$\delta_k=\delta(I_k,\mu,\Delta)=\prod_i \delta(P_i,\mu,\Delta) \tag{20}$$

If $i=2$, then the density function was a two-variable Gaussian density function. The calculation of the covariance matrix and the correlation coefficient r was extremely complex. Therefore, supposing that there was no correlation between the two information structures, i.e. $r=0$. Supposing that two variables in Gaussian density function were noted as x and y , single Gaussian density function was calculated recursively as follows:

(1) If variable x and y had the same mean μ and standard deviation σ , then:

$$\begin{aligned}\rho_{(x,y)}&=\frac{1}{\sqrt{2\pi}\sigma\sqrt{(1-r^2)}}e^{-\frac{1}{2}[(\frac{(x-\mu)^2-2r(x-\mu)(y-\mu)+(y-\mu)^2}{2\sigma^2}]}\\&=\frac{1}{\sqrt{2\pi}\sigma}e^{-\frac{1}{2}(\frac{(x-\mu)^2+(y-\mu)^2}{2\sigma^2})}\end{aligned} \tag{21}$$

(2) If μ and σ were different, the joint density function was defined as:

This article has been accepted for publication in a future issue of this journal, but has not been fully edited. Content may change prior to final publication. Citation information: DOI 10.1109/JSEN.2016.2641501, IEEE Sensors Journal

$$\rho_{(x,y)} = \frac{1}{\sqrt{2\pi\sigma_x\sigma_y}\sqrt{(1-r^2)}} e^{-\frac{1}{2}[\frac{(x-y)^2-2r(x-\mu_x)(y-\mu_y)+(y-\mu_y)^2}{\sigma_x^2+\sigma_y^2}]} = \frac{1}{\sqrt{2\pi\sigma_x\sigma_y}} e^{-\frac{1}{2}(\frac{(x-\mu_x)^2+(y-\mu_y)^2}{\sigma_x^2+\sigma_y^2})} \tag{22}$$

C. PEO-GMM

For time-series based image fusion, it was compulsory to calculate all of I_k's density functions and calculate the new density function. For m images, let $I_{fusion} = \sum_{i=1}^{m} \alpha_i \delta(P, \mu_i, \Delta_i)$, for a normalized weight parameter α, i.e., $\sum_i \alpha_i = 1$. To calculate and simplify the covariance matrix Δ, let

$$\Delta = \begin{bmatrix} \sigma^2 & 0 & \cdots & 0 \\ 0 & \sigma^2 & \cdots & 0 \\ 0 & \cdots & \cdots & 0 \\ 0 & 0 & \cdots & \sigma^2 \end{bmatrix} = \sigma^2 \vec{I} \tag{23}$$

From the SGM, it was obtained that:

$$\delta(P, \mu, \sigma^2\vec{I}) = \frac{1}{\sqrt{(2\pi)^3}} \sigma^{-1} e^{-\frac{(P-\mu)^T(P-\mu)}{2\sigma^2}} \tag{24}$$

For calculating μ and Δ, Expectation Maximization (EM) algorithm was applied, and we used Lagrange multiple (LM) to make partial derivative of μ and Δ on Eq. (24), and the following expressions were obtained respectively:

$$\begin{aligned} \partial_\mu[\delta(P,\mu,\sigma^2\vec{I})] &= \frac{1}{\sqrt{(2\pi)^3}} \partial_\mu(\sigma^{-1} e^{-\frac{(P-\mu)^T(P-\mu)}{2\sigma^2}}) \\ &= \frac{1}{\sqrt{(2\pi)^3}} \sigma^{-1} e^{-\frac{(P-\mu)^T(P-\mu)}{2\sigma^2}} \partial_\mu(-\frac{(P-\mu)^T(P-\mu)}{2\sigma^2})) \\ &= \delta(P,\mu,\sigma^2\vec{I})(\frac{P-\mu}{\sigma^2}) \end{aligned} \tag{25}$$

Continuously, making partial derivative of Δ on Eq. (24), we had that,

$$\begin{aligned} \partial_\Delta[\delta(P,\mu,\sigma^2\vec{I})) &= \frac{1}{\sqrt{(2\pi)^3}}((-1)\sigma^{-2} e^{-\frac{(P-\mu)^T(P-\mu)}{2\sigma^2}}) \\ &+ \frac{1}{\sqrt{(2\pi)^3}} \sigma^{-1} e^{-\frac{(P-\mu)^T(P-\mu)}{2\sigma^2}} [\frac{(P-\mu)^T(P-\mu)}{\sigma^3}] \\ &= \delta(P;\mu,\sigma^2\vec{I})(\frac{(P-\mu)^T(P-\mu)}{\sigma^3} - \frac{1}{\sigma^2}) \end{aligned} \tag{26}$$

By continuing this process along with the proposed Lagrange multipliers, then, for $\Delta = c\vec{I}$, $c \in R$, GMM was defined as $G(P) = \sum_i \alpha_i \delta(P, \mu_i, \sigma_i)$, $i = 1, 2, \cdots, lf$. The number of parameters for estimation is $3l$. Let $\theta = [\alpha_1, \alpha_2, \cdots, \alpha_l, \mu_1, \mu_2, \cdots \mu_l, \sigma_1^2, \sigma_2^2, \cdots, \sigma_l^2]$, the object was that:

$$\begin{aligned} L(\theta) &= \ln[\prod_i G(P_i)] \\ &= \sum_i \ln(GP_i)) \\ &= \sum_i \ln(\sum_{j=1}^{l} \alpha_1 \delta(P_i, \mu_j, \sigma_j^2)) \end{aligned} \tag{27}$$

, which could be differentiated w.r.t. μ_j and σ_j. Thus, we had that:

$$\partial_{\mu_j}(L(\theta)) = \sum_i \frac{\alpha_j \delta(P_i, \mu_j, \sigma_j^2)}{\sum_{j=1}^{l} \alpha_i \delta(P_i, \mu_j, \sigma_j^2)} \frac{P_i - \mu_j}{\sigma_j^2} \tag{28}$$

Let $\varphi_j(P_i) = \frac{\alpha_j \delta(P_i, \mu_j, \sigma_j^2)}{\sum_{j=1}^{l} \alpha_j \delta(P_i, \mu_j, \sigma_j^2)}$, so that:

$$\partial_{\mu_j}(L(\theta)) = \sum_i \varphi_j(P_i)(\frac{P_i - \mu_j}{\sigma_j^2}) \tag{29}$$

Similarly, we can find:

$$\begin{aligned} \partial_{\sigma_j}(L(\theta)) &= \sum_i \frac{\alpha_j \delta(P_i; \mu_j, \sigma_j^2)}{\sum_{j=1}^{l} \alpha_i \delta(P_i; \mu_j, \sigma_j^2)} \\ &\cdot [\frac{(P_i - \mu_j)^T (P_i - \mu_j)^T}{\sigma_j^3} - \frac{1}{\sigma_j^2}] \\ &= \sum_i \varphi_j(P_i)[\frac{(P_i - \mu_j)^T (P_i - \mu_j)^T}{\sigma_j^3} - \frac{1}{\sigma_j^2}] \end{aligned} \tag{30}$$

Setting the above two equations equal to 0, we had

$$\hat{\mu}_j = \frac{\sum_i \varphi_j(P_i) P_i}{\sum_i \varphi_j(P_i)} \tag{31}$$

$$\hat{\sigma}^2 = \frac{1}{3} \frac{\sum_i \varphi_j(P_i)(P_i - \mu_j)^T (P_i - \mu_j)}{\sum_i \varphi_j(P_i)} \tag{32}$$

For α_j, under the constraint $\sum_j \alpha_j = 1$, we used Lagrange multipliers to re-define the object as

$$\begin{aligned} J &= L(\theta) + \lambda(1 - \sum_{i=1} \alpha_i) \\ &= \sum_i \ln(\sum_j \alpha_j \delta(P_i, \mu_j, \sigma_j^2)) + \lambda(1 - \sum_{i=1} \alpha_i) \end{aligned} \tag{33}$$

Differentiating this new object w.r.t. α_j, thus:

$$\partial_{\alpha_j} J = \sum_i \frac{\delta(P_i, \mu_j, {\sigma_j}^2)}{\sum_{j=1}^{l} \alpha_j \delta(P_i, \mu_j, {\sigma_j}^2)} - \lambda$$
$$= \frac{1}{\alpha_j} \sum_i \varphi_j(P_i) - \lambda \quad (34)$$
$$= 0$$

$$[\hat{\alpha_1}, \alpha_2, \cdots \alpha_l] = [\frac{1}{\lambda}\sum_i \varphi_1(P_i)], \frac{1}{\lambda}\sum_i \varphi_2(P_i), \cdots \frac{1}{\lambda}\sum_i \varphi_k(P_i)] \quad (35)$$

$$\hat{\alpha_1} + \alpha_2 + \cdots + \alpha_l = \frac{1}{\lambda}(\sum_i (\varphi_1(P_i) + \varphi_2(P_i) + \cdots + \varphi_k(P_i)) = 1 \quad (36)$$

We know $\lambda = l$, so:

$$[\hat{\alpha_1}, \alpha_2, \cdots \alpha_l] = [\frac{1}{lf}\sum_i \varphi_1(P_i)], \frac{1}{l}\sum_i \varphi_2(P_i), \cdots, \frac{1}{l}\sum_i \varphi_k(P_i)] \quad (37)$$

, where φ is also a function of parameters,

In actuality, the density function of information fusion under this special structure is a product of the fusion of SGMs. For all images I_k and their SGM densities $\delta(I_k)$, the image fusion result was finally obtained using the GMM after parameter estimation, so for m images, we had that,

$$\prod_k \delta(I_k) = \prod_k \frac{1}{\sqrt{(2\pi)^3}\sigma_k} e^{-\frac{1}{2\sigma_k^2}(P-\mu)^T(P-\mu)}$$
$$= \frac{1}{\sqrt{(2\pi)^{3m}}\prod_k \sigma_k} e^{\sum_k -\frac{1}{2\sigma_k^2}(P-\mu)^T(P-\mu)}$$
$$= \frac{1}{\sqrt{(2\pi)^{3m}}\prod_k \sigma_k} e^{\alpha P^2 + \beta P + \gamma} \quad (38)$$
$$= \frac{1}{\sqrt{(2\pi)^{3m}} \cdot C \cdot \prod_k \sigma_k} e^{-\frac{1}{2\sigma_k^2}(P'-\mu')^T(P'-\mu')}$$
$$= C'\delta$$

, where, C' was calculated by expanding the index of e using binomial theorem. In particular, in a one-dimensional space with $\sigma = 1$, it was obtained that:

$$\delta(I_{fusion}) = \frac{1}{\sqrt{(2\pi)^{3m}}\prod_k \sigma_k} e^{\alpha x^2 + \beta x + \gamma}$$
$$= \frac{1}{\sqrt{(2\pi)^{3m}}} e^{\alpha x^2 + \beta x + \gamma}$$
$$= \frac{1}{\sqrt{(2\pi)^{3m}}} e^{x'^2 + \beta' x' + \gamma'} \quad (39)$$
$$= C\frac{1}{\sqrt{(2\pi)^3}} e^{(x'-\mu)^2}$$

, where C also was calculated by expanding the index of e using binomial theorem. This was a linear transformation of the basic Gaussian function. Thus, for any two image sets I_i and I_j, the result of fusion could be written as $I_{ij} =< P_{ij}, \mu_{ij}, \Delta_{ij} >$.

In experimental stage, Matlab R2014b was used to develop the PEO- GMM fusion algorithm in this research, and the pseudo-code was given as follows:

FUNCTION[Alpha, Mu, Data]
//Alpha is array of each fusing parameters of Gaussian function
//Mu is the mean of variables
//Data is input data
//output F= Pxi*Alpha' which Pxi was calculated by Gaussian PDF function

1. loglik_threshold ← 1E-10; // Set EM criterion for stopping iteration of algorithm
2. // PARAMETER INITIALIZATION
2.1 [dim, N]←size(Data); M←size(Mu0,2)
2.2 loglik_old←realmax; nbStep←0
2.3 Mu←Mu0; Sigma←Sigma0
2.4 Alpha←Alpha0; Epsilon←0.0001
3. //----E STEPS--
3.1 FOR i←1::M
3.2 Pxi(:,i)←Gauss_PDF(Data, Mu(:,i), Sigma(:,:,i))
3.3 **CALCULATING PDF OF EACH POINT**
3.4 END FOR
4. // COMPUTING POSTERIOR PROBABILITY BETA(I|X)
4.1 Pix_tmp ← repmat(Alpha,[N 1]).*Pxi;
4.2 Pix←Pix_tmp ./ (repmat(sum(Pix_tmp,2),[1 M])+realmin);
4.3 Beta ← sum(Pix);
5. // M-STEPS
5.1 FOR i←1::M
5.2 Alpha(i) ← Beta(i) / N; //UPDATE
5.3 Mu(:,i) ← Data*Pix(:,i) / Beta(i); **//MEAN UPDATE**
5.4 Data_tmp1 ← Data_repmat(Mu(:,i),1,N); **// SQR UPDATE**
5.5 Sigma(:,:,i) ← (repmat(Pix(:,i)',dim, 1) .* Data_tmp1*Data_tmp1') / Beta(i);
5.6 Sigma(:,:,i) ← Sigma(:,:,i) + 1E-5.*diag(ones(dim,1)); **//ADD A TINY VARIANCE TO AVOID NUMERICAL INSTABILITY**
5.7 END FOR
6.//STOPPING CRITERION
6.1 FOR i←1:M
Pxi(:,i) ← GaussPDF(Data, Mu(:,i), Sigma(i));
//COMPUTE THE NEW PROBABILITY P(X|I)
6.2 END FOR
6.3 F ← Pxi*Alpha';
6.4 F(find(F<realmin)) ← realmin;
6.5 loglik = mean(log(F)); **//COMPUTE THE LOG LIKELIHOOD**
7. //STOP THE PROCESS DEPENDING ON THE INCREASE OF THE LOG LIKELIHOOD
7.1 IF abs((loglik/loglik_old)-1) < loglik_threshold
7.2 BREAK;
7.3 END IF
8. loglik_old ← loglik;

This article has been accepted for publication in a future issue of this journal, but has not been fully edited. Content may change prior to final publication. Citation information: DOI 10.1109/JSEN.2016.2641501, IEEE Sensors Journal

And the pseudo-code of Gaussian PDF as follow,

FUNCTION GaussPDF[Data, Mu, Sigma]
// CALCULATING PROBABILITY DENSITY FUNCTION (PDF) OF EACH GROUP DATA FOLLOWING THE NORMAL DISTRIBUTION
Input: Data: DxN, N D-dimensional data; Mu: D x 1,M initial value of centers of Gauss model
Sigma: M x M , variance of each Gaussian model
Output: prob: 1 x N array representing the probabilities for the N data-points.

1. [dim,N] = size(Data) // **GET DIM AND N**
2. Data ← Data' - repmat(Mu',N,1); // **REPEAT MATRIX BY COPY AND TILE**
3. prob ← sum((Data*inv(Sigma)).*Data, 2) // **"INV" MEANS INVERSE MATRIX**
4. prob ← exp(-0.5*prob) / sqrt((2*pi)^dim * (abs(det(Sigma))+realmin)) // **DET MEANS DETERMINANT, ABS MEANS ABSOLUTE VALUE, SQRT MEAN SQUARE ROOT CALCULATIONS**

In addition, the proposed PEO-GMM for time-series based image dataset was given by:

FUNCTION[img1, img2] : IMPROVED GAUSSIAN MIXED FUSION
// img1 and img2 are dataset of the same region of interest in different time

1. PREPROCESS FOR THE IMAGES
2. LAPLACIAN GAUSSIAN FILTER
2.1 img1←LoG[img1]
2.2 img2←LoG[img2]
3. DISCRETE WAVELET TRANSFORM
3.1 img1←DWT[img1]
3.2 img2←DWT[img2];
3.3 x1←img1.x; y1←img1.y
3.4 x2←img2.x; y2←img2.y
4. CALCULATE THE MEAN AND STANDARD DEVIATION
4.1 mean_x1←MEAN[x1]; mean_y1←MEAN[y1]
4.2 mean_x2←MEAN[x2]; mean_y2←MEAN[y1]
4.3 Sigma_x1←SIG[x1]; Sigma_y1←SIG[y1]
4.4 Sigma_x1←SIG[x2]; Sigma_y2←SIG[y2]
5. PARAMERIAZED IMPROVED GAUSSIAN MIXED FUSION
5.1
G_1←EXP[0.5*[SQRT[[x1-Mean_x1]^2+[x2-mean_x2]^2]/Sigma_x1*Sigma_x2];
5.2
G_2←EXP[0.5*[SQRT[[y1-Mean_y1]^2+[y2-mean_y2]^2]/Sigma_y2*Sigma_y2];
5.3 img[G]←[G_1, G_2]; // **STORAGE G_1 AND G_2 MEANS THE IMAGE PIXEL IS G_1 IN X AND G_2 IN Y**
6. INVERSE DWT
6.1 G←iDWT[G];

These proposed pseudo-codes for the PEO-GMM function for image fusion were compared to other fusion algorithms. Assume two time-series plantar pressure images presented by 2 matrices A and B, thus the fusion algorithm was composed of the calculation process such as Max-UD (Upper-Down), which introduced by the following Up-Down fusion code [41]:

UP-DOWN FUSION[A, B]

1. 'max' : D ← abs(A) >= abs(B) ; C ←A(D) + B(~D)
2. - 'min' : D ←abs(A) <= abs(B) ; C ← A(D) + B(~D)
3. - 'mean' : C ← (A+B)/2 ; D ←ones(size(A))
4. Up-Down fusion, with paramMETH >= 0 // A GIVEN THRESHOLD FOR PARAMETER-DEPENDENT -FUSMETH
4.1 x ← linspace(0,1,size(A,1));
4.2 P ← x.^paramMETH;
4.3 // THEN EACH ROW OF C IS COMPUTED WITH:
4.4 C(i,:) ←A(i,:)*(1-P(i)) + B(i,:)*P(i);
4.5 So C(1,:) ← A(1,:) and C(end,:)= B(end,:)

D. Image Quality Evaluation for the Fusion Result

Supposed that $A(i,j)$ and $B(i,j)$ were the source images, $R(i,j)$ was the reference image, and $F(i,j)$ was the fusion image, where $(i,j) \in [1,N] \times [1,M]$. The indices for full information evaluation referred to source image and to reference image, the evaluation of the difference with the reference image, and the evaluation of the difference with the source image were calculated by the following metrics.

1) Full Information Evaluation

- The mean was defined as the average grey of the image that was calculated by:

$$M = \frac{1}{NM}\sum_{i=1}^{N}\sum_{j=1}^{M} grey(F(i,j)) \tag{40}$$

- The standard deviation was defined as the difference of each point in the image and the mean value, which was given by:

$$SD = \sqrt{\frac{1}{NM}\sum_{i=1}^{N}\sum_{j=1}^{M}(F(i,j)-M)} \tag{41}$$

- In this paper, the entropy was image entropy which represented the aggregation characteristics of image gray level distribution. Since the single grey point was independent, the image gray distribution $P = \{P_0, P_1, \cdots P_K\}$, in which P_k represented the probability of the gray value of image pixel was k in $F(i,j)$, thus the entropy was given by:

$$E = -\sum_{i=0}^{L-1} P_i \log_2 P_i \tag{42}$$

- The average gradient reflected the ability to change the contrast and texture features of the image. For a single image, the gray value of each pixel could be considered. Its formula was given by:

$$AG = \frac{1}{NM}\sum_{i=1}^{N}\sum_{j=1}^{M}\sqrt{\frac{\Delta P_x + \Delta P_y}{2}} \tag{43}$$

, where, L was the total grey levels of the image.

- The spatial frequency, which was a characteristic of any periodic structure across its position in space and was used to measure the overall activity level of an image, was given by:

$$SF = \sqrt{\left(\frac{1}{NM}\sum_{i=1}^{N}\sum_{j=2}^{M}[I(i,j)-I(i,j-1)]^2\right)^2 + \left(\frac{1}{NM}\sum_{j=1}^{M}\sum_{i=2}^{N}[I(i,j)-I(i-1,j)]^2\right)^2} \tag{44}$$

2) Indices Relative to Reference Image

In some fields, the existing standard reference image was normally used to evaluate the efficiency of the fusion result, so as to the plantar pressure distribution images in experiment stage, we also selected a standard reference image to evaluate the result. As time-series based plantar image fusion was operating, the reference image was necessary. However, it was difficult to be acquired, so we collected all plantar pressure images from Footscan 7's average imaging function. It was to average of the calculated pressure under specific calculated foot regions for different measurements. This could be useful

to find the average pressure loadings for a group of subjects. Also, it could be used to look at the repeatability of a specific movement. So in FWES, reference image relative indices were also used as a weight for the system as follows:

- The root mean square error was given by:

$$RMS = \sqrt{\frac{1}{NM}\sum_{i=1}^{N}\sum_{j=1}^{M}[R(i,j)-F(i,j)]^2} \quad (45)$$

- The signal to noisy rate, which means comparing the level of a given signal to the level of background noise, was calculated by:

$$SNR = 10\lg\frac{\sum_{i=1}^{N}\sum_{j=1}^{M}F^2(i,j)}{\sum_{i=1}^{N}\sum_{j=1}^{M}[R(i,j)-F(i,j)]^2} \quad (46)$$

- The peak signal to noise ratio, which was the ratio between the maximum possible power of a signal and the power of corrupting noise, was calculated by:

$$PSNR = 10\lg\frac{(L-1)^2}{\sum_{i=1}^{N}\sum_{j=1}^{M}[R(i,j)-F(i,j)]^2} \quad (47)$$

3) Indices Relative to the Source Image

- The mean cross entropy used for calculating the difference of the gray distribution of the two images was expressed by:

$$MCE = \frac{1}{2}\left(\sum_{i=0}^{L-1}P_{A_i}\log_2\frac{P_{A_i}}{P_{F_i}} + \sum_{i=0}^{L-1}P_{B_i}\log_2\frac{P_{B_i}}{P_{F_i}}\right) \quad (48)$$

,where P_{A_i} is gray distribution of image A_i and the same to B_i and F_i (fused image)

- The joint entropy, which measured the uncertainty associated with a set of variables, was expressed by:

$$JE_{F,A} = \sum_{i=0}^{L-1}\sum_{j=0}^{L-1}P_{F,A}(i,j)\log P_{F,A}(i,j) \quad (49)$$

, where, $P_{F,A}(i,j)$ is joint gray histogram of image A and F.

- The mutual information; a measure of the mutual dependence between the two variables, was expressed by:

$$MI((A,B)->F) = \sum_{i=0}^{L-1}\sum_{j=0}^{L-1}\sum_{k=0}^{L-1}P_{A,B,F}(i,j,k)\log_2\frac{P_{A,B,F}(i,j,k)}{P_{A,B}(i,j)P_F(k)} \quad (50)$$

, where, $P_{A,B,F}$ is joint gray histogram of image A, B and F.

- The deviation index, which presents the matching degree of information entropy of the spectral of fusion image and the original image, was expressed by:

$$DI = \frac{1}{2NM}\left(\sum_{i=1}^{N}\sum_{j=1}^{M}\frac{|F(i,j)-A(i,j)|}{A(i,j)} + \sum_{i=1}^{N}\sum_{j=1}^{M}\frac{|F(i,j)-B(i,j)|}{B(i,j)}\right) \quad (51)$$

- The correlation coefficient, which presented the relationship between the two variables and their relative directions, was expressed by:

$$CC = \frac{1}{2}\left[\frac{\sum_{i=1}^{N}\sum_{j=1}^{M}[F(i,j)-M_F][A(i,j)-M_A]}{\sqrt{\sum_{i=1}^{N}\sum_{j=1}^{M}[F(i,j)-M_F]^2[A(i,j)-M_A]^2}} + \frac{\sum_{i=1}^{N}\sum_{j=1}^{M}[F(i,j)-M_F][B(i,j)-M_B]}{\sqrt{\sum_{i=1}^{N}\sum_{j=1}^{M}[F(i,j)-M_F]^2[B(i,j)-M_B]^2}}\right] \quad (52)$$

- The degree of distortion that reflects the distortion degree of the spectrum of the fusion image was expressed by:

$$DD = \frac{1}{2NM}\left[\sum_{i=1}^{N}\sum_{j=1}^{M}|F(i,j)-A(i,j)| + \sum_{i=1}^{N}\sum_{j=1}^{M}|F(i,j)-B(i,j)|\right] \quad (53)$$

4) Fuzzy Weighted Evaluation System

The fuzzy weighted evaluation system involved all these indices mentioned in Section III.D 1)-3) . In the current work, the weight of fuzzy comprehensive analysis was determined using the following methods:

- Method for field experts: determination of weight was calculated by the frequency statistics methodbyassigning factor set for the object. Afterward, giving this set to a certain number of experts to put forward their own weight distribution. Then, organize the recyclingweight after the questionnaire for each factor to carry out a single factor statistical experiment.
- Method for indices: using fuzzy analytic hierarchy process (AHP) to determine the weight. This method was a very useful for multiple criteria decision-making in fuzzy environments and the method from the hierarchy structure of comprehensive evaluation system of indicators for each criterion on the same level indicators was pair-wise compared. Moreover, using psychological scale, such as Likert Scale (a common psychometric scale in questionnaire systems) to construct judgment matrix, and solving the largest eigen-values and corresponding eigen-vectors, afterward the weight vector was normalized.

In the current study, a fused image was required to achieve high entropy and low RMSE. Thus, two type indices were proposed, namely i) for the positive evaluation with higher value noted as Q', and ii) for negative evaluation with low value, such as the RMSE and PNSR noted as Q, given by:

$$f_1 = \sum_{i=1}^{R}\xi_i Q_i^{'},\ f_2 = \sum_{i=1}^{S}\eta_i Q_i \quad (54)$$

, where ξ_i and η_i were the weights of filed experts. Consequently, f_i reflects the image quality of fusion result

This article has been accepted for publication in a future issue of this journal, but has not been fully edited. Content may change prior to final publication. Citation information: DOI 10.1109/JSEN.2016.2641501, IEEE Sensors Journal

using the proposed method (Gaussian mixed operator) along with higher f_1 and lower f_2. In the current work, f_1 involved $\{M, E, AG, SF, JE, MI, CC\}$ and f_2 involved $\{SD, RMSE, SNR, PSNR, MCE, DI, DD\}$. These indices were used in the comparative analysis of the proposed fusion approach.

IV. Results and Discussion

The proposed Gaussian mixed operator approach was carried out using 2 - level Haar wavelet. The approximation coefficients and details coefficient were defined by the proposed user-defined Gaussian mixed fusion algorithms. Figure 2 illustrates the original two images for the fusion process and their Laplacian Gaussian filter. The experiment included image set of the original images, gray images, Gaussian Laplace filter applied to the images using Gaussian mixed fusion and the up-down fusion. The Footscan 7.0 system of RSscan international was used to obtain foot pressure distribution dataset. And Table I shows the details of the measurement of the system. A total of 20 students were involved in the 10 minutes test and the data was acquired. Hence, the used images in the current study were obtained from pressure sensors.

Table 1. the performance of pressure sensors capturing system

Items	**Measurement**		
Area	40*50 cm^2	Total sensors	4096
Numbers of sensor	4 per cm^2	Sampling Hz	125-300hz
Size of each sensor	0.5*0.7 cm^2	analog channels	16
Image resolution	12 bits	Entry level	2m

The local pressures under the foot during unroll of the foot were obtained. Furthermore, the system could provide the pressure information based on the automatic calculated zones under the foot. It could also be localized under small spots under the foot.

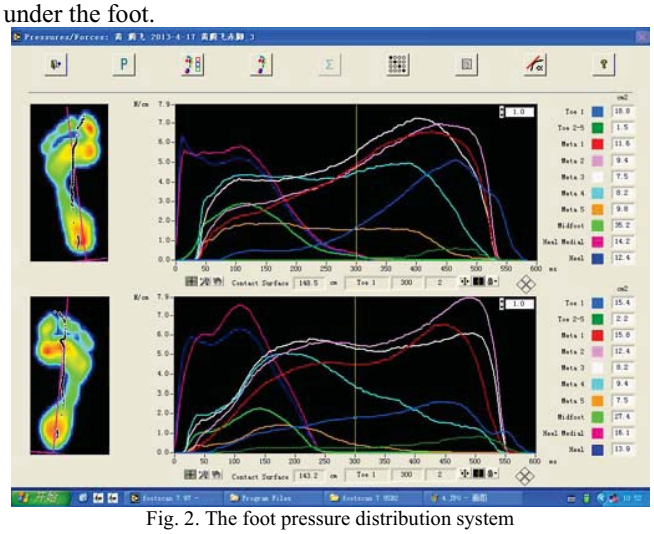

Fig. 2. The foot pressure distribution system

Initial images and their LoG filtered images were obtained, as shown in Figure 3.

(a) (b) (c) (d)

Fig. 3. Images set: (a , b) the initial images, and (c, d) the Laplacian Gaussian filter for the initial images

Then, the fusion started operating as proposed in Section III. Figure 4 shows the result of using PEO-GMM and the initial images.

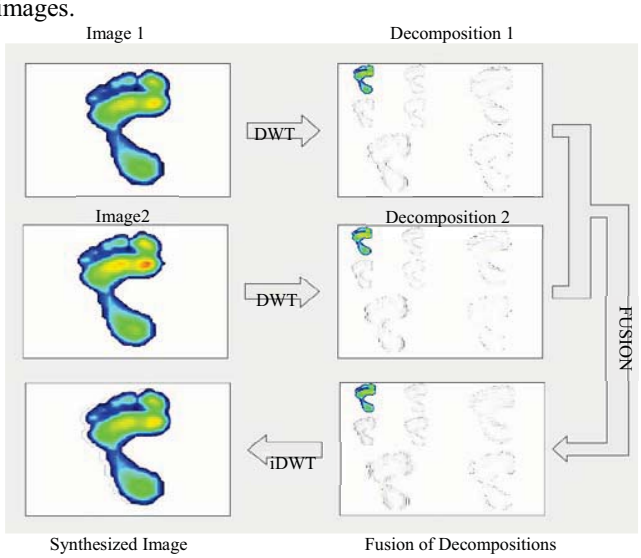

Fig.4. The initial images and its synthesized image under PEO-GMM

Continuously, Fig. 5 demonstrates the results of the proposed fusion method in the case of using the gray images.

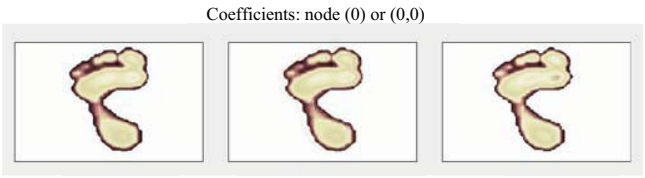

Fig. 5. The Initial gray images and their synthesized image with Gaussian Mixed Fusion

Furthermore, the Gaussian Laplace filter for the initial images was applied and the synthesized image was obtained using the PEO-GMM as demonstrated in Figure 6.

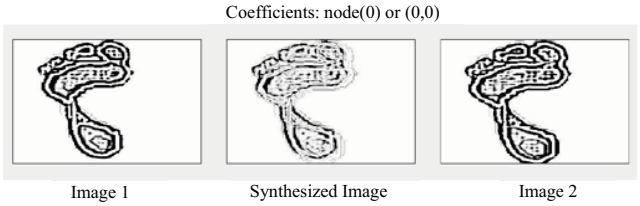

Fig. 6. LoG applied images with Gaussian fusion

For the comparative analysis, the MEAN-MEAN, MAX-MIN and Up-Down (UD) fusion for LoG images were applied to the same image set of LoG filtering images as demonstrated in Figure 7.

This article has been accepted for publication in a future issue of this journal, but has not been fully edited. Content may change prior to final publication. Citation information: DOI 10.1109/JSEN.2016.2641501, IEEE Sensors Journal

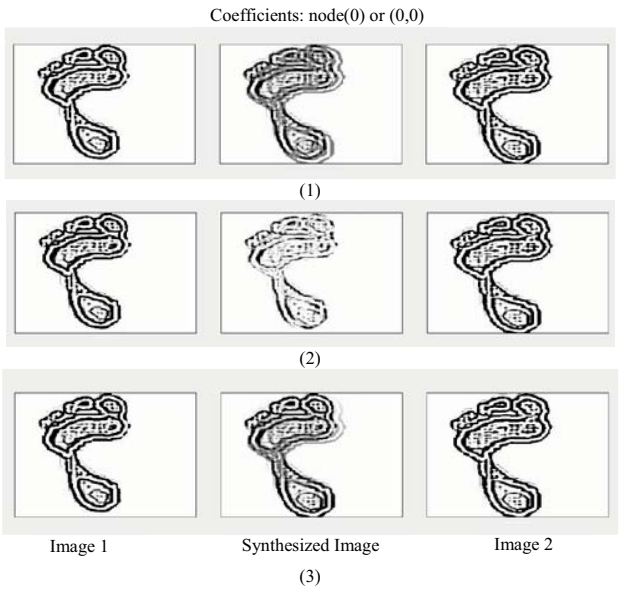

Fig. 7. The MEAN-MEAN fusion (1) MAX-MIN fusion (2) and UP-DOWN fusion (3) for LoG images

Now, the indices calculations were started to evaluate the synthesized images under these conditions using f_1 and f_2 in order to show the significant progress of the proposed method.

The performance evaluation of the proposed approach was measured by using the proposed indices in Sect. II.D.4 which was used to evaluate the result images' quality. In addition, a comparative analysis was reported to show the effectiveness of the proposed method. The evaluation indices, namely f_1 included M, E, AG, AF, UE, MI, CC and f_2 included SD, RMSE, SNR, PSNR, CE, DI, DD, were calculated. The positive indices f_1 and the negative indices f_2 for the synthesized image using different fusion operator were tabulated in Table 2.

Table 2. The indices for a GM fusion based synthsized image

f1/images	M	E	AG	AF	JE	MI	CC
Initial image	0.87	2.7	2.24	8.15	3.77	1.88	0.55
Gray image	0.77	2.5	2.02	7.51	3.21	1.8	0.47
LoG image	**0.92**	**2.92**	**2.74**	**9.11**	**3.92**	**2.28**	0.52
f2/images	**SD**	**RMSE**	**SNR**	**PSNR**	**MCE**	**DI**	**DD**
Initial image	0.15	0.44	1.26	1.24	4.52	5.23	1.74
Gray image	0.09	0.48	1.17	1.1	4.77	7.21	2.26
LoG image	**0.07**	**0.41**	**1.07**	1.15	**4.34**	5.07	1.88

Table 2 depicts that the synthsized image using the LoG approach has supperior evaluation indices compared to the original (initial) and the gray images. The proposed LoG fusion approach established its efficiency by achieving the maximum values of the M, JE, MI, and CC as well as the minimum values of the SD, RMSE, SNR, MCE, and the DI.

In addition, 20 pairs of images for fusion using up-down (UP-DOWN_FUSION), max-min (MAX_MIN), mean-mean (MEAN-MEAN) and PEO-GMM, and entropy (E) and room mean standard error (RMSE) were selected as representation of the positive and negative indices as reported in Table 3.

Table 3. The 20 pairs typical indeces for the different fusion algorithm

	UP-DOWN_FUSION		**MAX-MIN_FUSION**		**MEAN_MEAN**		**PEO-GMM_FUSION(*)**	
	E	RMSE	E	RMSE	E	RMSE	E	RMSE
LAB1	1.75	0.3	2.1	0.24	2.14	0.3	2.55	0.31
LAB2	1.42	0.15	2.12	0.22	2.35	0.21	2.21	0.17
LAB3	1.62	0.23	2.2	0.35	1.25	0.55	2.56	0.22
LAB4	2.13	0.23	2.33	0.3	2.17	0.3	2.45	0.21
LAB5	1.45	0.21	1.55	0.24	2.1	0.21	2.47	0.17
LAB6	2.3	0.15	1.25	0.23	2.35	0.22	2.05	0.11
LAB7	2.55	0.29	2.3	0.38	2.1	0.4	1.98	0.41
LAB8	2.02	0.25	2.17	0.26	1.47	0.17	2.11	0.15
LAB9	1.25	0.42	2.2	0.44	1.24	0.4	1.88	0.4
LAB10	2.2	0.4	2.44	0.35	1.25	0.33	2.25	0.35
LAB11	2.1	0.53	2.1	0.22	1.78	0.12	2.67	0.1
LAB12	1.98	0.42	2.24	0.26	2.22	0.12	2.88	0.07
LAB13	2.21	0.22	1.76	0.21	2.54	0.18	2.76	0.15
LAB14	2.21	0.3	2.4	0.37	2.58	0.44	2.57	0.42
LAB15	1.55	0.35	2.37	0.45	2.35	0.55	2.02	0.33
LAB16	2.01	0.3	2.79	0.23	2.66	0.19	3.35	0.27
LAB17	2.02	0.26	2.1	0.35	2.5	0.2	2.45	0.18
LAB18	2.22	0.25	2.23	0.38	2.1	0.33	1.88	0.35
LAB19	2.01	0.32	2.08	0.32	1.22	0.32	2.21	0.31
LAB20	1.26	0.32	1.38	0.31	1.2	0.27	2.1	0.26

This article has been accepted for publication in a future issue of this journal, but has not been fully edited. Content may change prior to final publication. Citation information: DOI 10.1109/JSEN.2016.2641501, IEEE Sensors Journal

Table 3 depicts that the PEO-GMM achived the least average RMSE of value 0.25 and the highest average entropy of 2.38 value. The same results are illustrated in Figures 8 and 9 representing the entropy and the RMSE; respectively for the different fusion methods based on log filtering.

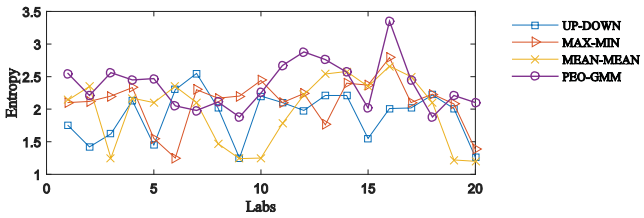

Fig. 8. The entropy for different fusion method based on log filtering

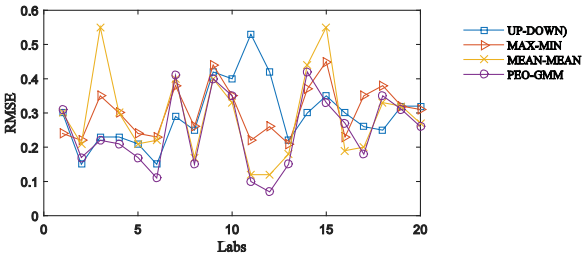

Fig. 9. The RMSE for different fusion methods based on log filtering

The visilized entropy indices in Figures 8 and 9, for comparing the proposed GM_fusion approach to the up-down, min-max and mean- mean fusion methods, established that the proposed PEO-GMM method achieves entropy of 80% or higher than the other methods, and RMSE of about 85% or lower than the other methods. Moreover, Figures 10 and 11 demonstrate the fuzzy weighted positive indices f_1 and the negative indices f_2 for the different fusion methods.

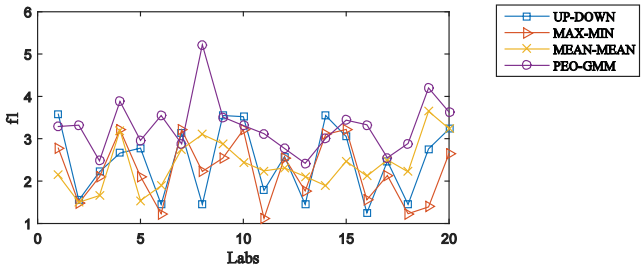

Fig. 10. The fuzzy weighted indice f_1 for the different fusion methods

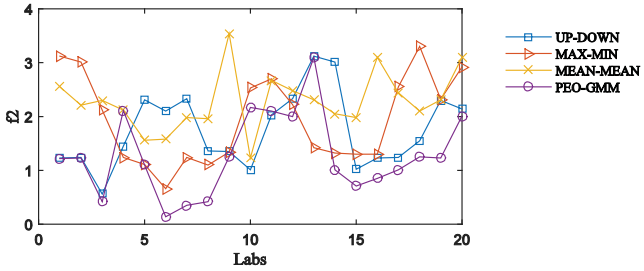

Fig.11. The fuzzy weighted indice f_2 for the different fusoion methods

Figures 10 and 11 illustrate the fuzzy weighted operation with f_1 and f_2 indices; respectively, which established that the proposed approach gains the outstanging results, where 90% value was obtained for f_1 (the highest compared to the other methods) and the lowest value of 85% was obtained for f_2 compared to the other methods.

The proposed method can be considered as apotential research direction on plantar pressure image recognition in [42] [43], especially for diabetic plantar research [44] in future works. Thus, diabetic plantar can be furthermore clustered and segmented the synthsized images shown in Figure 11, where 7-9 parts locate all fundamental points and produce fitable shoes for diabetic plantar as a future scope.

(1) lined edge (2) area segmenting

Fig. 12. Clustering segmentation of 7 pieces for the synthsized images

Additionally, the proposed method was feasbile for the functional magnetic resonance imaging (fMRI) dataset processing. This can open new research directions on tumor image segmentation in the medical domain. Researchers have already expressed their interest in the medical image processing applications [45][46][47]. In future work, time-series based images preprocesing can be improved as pixel or Gaussian pyramid operation based algorithms before fusion. Moreover, the weighted system also requires improvement. The adaptive neuro network fuzzy inference system (ANFIS) can be applied to train the fusion parameters and the weights and to get better quality result images. On the other hand, the proposed methods such as PEO-GMM and fuzzy weighted evalaution system can be applied in medical images like fMRI dataset and multi sensor fusion relatied research.

V. Conclusion Remarks

In this study, a novel LoG filtering with Gaussian Mixed (GM) operator based image fusion framework wasapplied for foot plantar imaging. The results showed that the proposed approachachieved superior performance compared to other filtering and fusion methods for the foot plantar imaging data set. The quality of the synthsized images were taken on fuzzy weighted indices based on evaluation system including 7 positive indices and 7 negative indices. Higher positve indices such as entropy with lower negative indices such as RMSE established outperforming results for the synthsized images as proved by the comparative analysis. The contribution of the current work are:

1) A gaussian mixed model was proved as more effective compared to the other fusion methods such as up-down, min-max and mean-mean for the plantar imaging fusion through indices system.

2) The synthsized image evaluation indices were totally involved and separated in positive and negative indices.

3) The fuzzy evaluation system was more accurate than the individual indices system employing weighted opertation.

The proposed approach gains entropy of 80% or higher than the other methods, and RMSE of about 85% or lower than the other methods. Moreover, the fuzzy weighted positive indices f_1 and the negative indices f_2 for the different fusion methods, where the proposed approach gained outstanging results, where 90% value is obtained for f_1 (the highest compared to the other methods) and the lowest value of 85% is obtained for f_2 compared to the other methods.The preceding results proved that the LoG filtering with Gaussian Mixed (GM) fusionoperator applied efficently for foot plantar imaging.

REFERENCES

[1] O. Cossairt, Tradeoffs and limits in computational imaging (Doctoral dissertation, Columbia University), 2011.

[2] J. A. Duro, J. A. Padget, C. R. Bowen, H. A. Kim, A. Nassehi, Multi-sensor data fusion framework for CNC machining monitoring, Mechanical Systems and Signal Processing, vol. 66, no.7, pp.505 -520, 2016.

[3] J. Dong, D. Zhuang, Y. Huang, J. Fu, Advances in Multi-Sensor Data Fusion: Algorithms and Applications, Sensors, vol. 9, pp.7771–7784, 2009

[4] GFortino, S. Galzarano, R. Gravina, W. Li, A framework for collaborative computing and multi-sensor data fusion in body sensor networks, Information Fusion, vol. 22, pp.50 – 70, 2015.

[5] W. Xu, J. Yu, A novel approach to information fusion in multi-source datasets: A granular computing viewpoint, Information Sciences, [online], available: 10.1016/j.ins.2016.04.009, 2016.

[6] Z.-J. Lu, Q. Xiang, L. Xu, An application case study on multi-sensor data fusion system for intelligent process monitoring, Procedia CIRP, //in: Variety Management in Manufacturing, Proceedings of the 47th CIRP Conference on Manufacturing Systems.vol. 17, pp.721 - 725, 2014.

[7] L. Dong, Q. Yang, H. Wu, H. Xiao, M. Xu, High quality multi-spectral and panchromatic image fusion technologies based on curvelet transform, Neurocomputing, vol. 159, pp. 268 -274, 2015.

[8] Y. Li, Y. Jiang, L. Gao, Y. Fan, Fast mutual modulation fusion for multi-sensor images, Optik- International Journal for Light and Electron Optics, vol. 126, no. 1, pp. 107 – 111, 2015.

[9] W.-T. Sung, K.-Y. Chang, Evidence-based multi-sensor information fusion for remote health care systems, Sensors and Actuators A: Physical, vol. 204, pp. 1 -19, 2013

[10] T. Tian, S. Sun, N. Li, Multi-sensor information fusion estimators for stochastic uncertain systems with correlated noises, Information Fusion, vol. 27, pp.126 – 137, 2016.

[11] W. He, W. Feng, Y. Peng, Q. Chen, G. Gu, Z. Miao, Multi-level image fusion and enhancement for target detection, Optik - International Journal for Light and Electron Optics 126 , (11-12) (2015) 1203 -1208.

[12] W. Zhi-she, Y. Feng-bao, P. Zhi-hao, C. Lei, J. Li-e, Multi-sensor image enhanced fusion algorithm based on NSST and top-hat transformation, Optik- International Journal for Light and Electron Optics,vol. 126, no.23,pp. 4184 – 4190, 2015.

[13] S. Kumar, R. M. Hegde, Multi-sensor data fusion methods for indoor localization under collinear ambiguity, Pervasive and Mobile Computing, [online]available: http://dx.doi.org/10.1016/j.pmcj.2015.09.001., 2016

[14] P. Mangalraj, A. Agrawal, Fusion of multi-sensor satellite images using non-subsampled contourlet transform, Procedia Computer Science, //in: eleventh International Conference on Communication Networks, ICCN 2015, August 21-23, 2015, Bangalore, India Eleventh International Conference on Data Mining and Warehousing, ICDMW 2015, August 21-23, 2015, Bangalore, India Eleventh International Conference on Image and Signal Processing, ICISP 2015, August 21-23, 2015, Bangalore, India. vol. 54, pp. 713 -720, 2015.

[15] Zairan Li, Ting He, Luying Cao, Tunhua Wu, Pamela McCauley, Valentina E. Balas and Fuqian Shi, Multi-source information fusion model in rule-based Gaussian-shaped fuzzy control inference system incorporating Gaussian density function, Journal of Intelligent & Fuzzy Systems, vol. 29, pp. 2335-2344, 2015.

[16] Z. Ji, Y. Xia, Q. Sun, Q. Chen, D. Feng, Adaptive scale fuzzy local gaussian mixture model for brain {MR} image segmentation, Neurocomputing, //in: special issue on the 2011 Sino-foreign-interchange Workshop on Intelligence Science and Intelligent Data Engineering (IScIDE 2011), Learning Algorithms and Applications Selected papers from the 19th International Conference on Neural Information Processing, ICONIP2012. vol. 134, pp. 60 - 69, 2014.

[17] H. Jiang, Y. Tian, Fuzzy image fusion based on modified self-generating neural network, Expert Systems with Applications,vol. 38, no.7,pp.8515-8523, 2011.

[18] I. Bloch, Fuzzy sets for image processing and understanding, Fuzzy Sets and Systems, //in: special Issue Celebrating the 50th Anniversary of Fuzzy Sets, vol. 281, pp. 280 - 291, 2015.

[19] C. Li, H. Duan, Information granulation-based fuzzy RBFNN for image fusion based on chaotic brain storm optimization, Optik - International Journal for Light and Electron Optics, vol. 126, no. 15-16, pp. 1400 -1406, 2015.

[20] S. Banerjee, D. Mukherjee, D. D. Majumdar, Fuzzy c-means approach to tissue classification in multimodal medical imaging, Information Sciences, vol. 115, no. 1-4, pp. 261 -279, 1999.

[21] B. V., K. H.K., Multi-modality medical image fusion using discrete wavelet transform, Procedia Computer Science, //in: proceedings of the 4th International Conference on Eco-friendly Computing and Communication Systems,vol.70, pp. 625 - 631, 2015.

[22] Yu Zhang, Xiangzhi Bai, Tao Wang, Boundary finding based multi-focus image fusion through multi-scale morphological focus-measure, Information Fusion, 35, 81-101, 2017

[23] Bingjian Wang, Jingya Hao, Xiang Yi, Feihong Wu, Min Li, Hanlin Qin, Hanqiao Huang, Infrared/laser multi-sensor fusion and tracking based on the multi-scale model, Infrared Physics & Technology, 75, 12-17, 2016

[24] P. Balasubramaniam, V. Ananthi, Image fusion using intuitionistic fuzzy sets, Information Fusion,20,21-30, 2014.

[25] T. Feng, S.-P. Zhang, J.-S. Mi, The reduction and fusion of fuzzy covering systems based on the evidence theory, International Journal of Approximate Reasoning, 53(1), 87- 103, 2012.

[26] N.L.W. Keijsers, N.M. Stolwijk, T.C. Pataky, Linear dependence of peak, mean, and pressure–time integral values in plantar pressure images, Gait & Posture, 31(1):140-142, 2010

[27] N.L.W. Keijsers, N.M. Stolwijk, J.W.K. Louwerens, J. Duysens, Classification of forefoot pain based on plantar pressure measurements, Clinical Biomechanics, 28(3): 350-356, 2013

[28] Lazarus Motha, Jiseok Kim, Woo Soo Kim, Instrumented rubber insole for plantar pressure sensing, Organic Electronics, 23, (2015), 82-86,

[29] U. H. Tang, R. Zgner, V. Lisovskaja, J. Karlsson, K. Hagberg, R. Tranberg, Comparison of plantar pressure in three types of insole given to patients with diabetes at risk of developing foot ulcers ?a two-year, randomized trial, Journal of Clinical & Translational Endocrinology 1 (4) (2014) 121 - 132.

[30] D.MC Janssen, A. P Sanders, N. A Guldemond, et al., A comparison of hallux valgus angles assessed with computerised plantar pressure measurements, clinical examination and radiography in patients with diabetes, Journal of Foot and Ankle Research 2014, 7:33-41

[31] Edmundas Kazimieras Zavadskas, Jurgita Antucheviciene, Seyed Hossein Razavi Hajiagha, et al., Extension of weighted aggregated sum product assessment with interval-valued intuitionistic fuzzy numbers (WASPAS-IVIF), Applied Soft Computing, Vol.24, pp.1013-1021, 2014

[32] Miguel Ángel Olvera-García, José J. Carbajal-Hernández, et al., Air quality assessment using a weighted Fuzzy Inference System, Ecological Informatics, Vol.33, pp.57-74, 2016,

[33] Marcin Relich, Pawel Pawlewski, A fuzzy weighted average approach for selecting portfolio of new product development projects, Neurocomputing,,http://dx.doi.org/10.1016/j.neucom.2016.05.104., 2016

[34] R. L. Joshi, T. R. Fischer, Comparison of generalized Gaussian and Laplacian modeling in DCT image coding, IEEE Signal Processing Letters, vol.2, no.5,pp. 81-82, 1995.

[35] H. Rabbani, R. Nezafat, S. Gazor, Wavelet-Domain Medical Image Denoising Using Bivariate Laplacian Mixture Model, IEEE Transactions on Biomedical Engineering, vol 56, no. 12, pp.2826-2837, 2009.

[36] Z. Miao, X. Jiang, K.-H. Yap, Contrast Invariant Interest Point Detection by Zero-Norm LoG Filter, IEEE Transactions on Image Processing, vol. 25, no. 1, pp. 331-342, 2016.

[37] F. Duan, L. Dai, W. Chang, et al., sEMG-Based Identification of Hand Motion Commands Using Wavelet Neural Network Combined With Discrete Wavelet Transform, IEEE Transactions on Industrial Electronics, vol. 63, no. 3, pp. 1923-1934, 2016.

[38] Z. Zhou, B. Wang, S. Li, M. Dong, Perceptual fusion of infrared and visible images through a hybrid multi-scale decomposition with Gaussian and bilateral filters, Information Fusion, vol. 30, pp. 15 – 26, 2016.
[39] W. Dou, S. Ruan, Y. Chen, D. Bloyet, J.-M. Constans, A frame- work of fuzzy information fusion for the segmentation of brain tumor tissues on MR images, Image and Vision Computing, vol. 25,no.2,pp. 164 - 171, 2007
[40] Ting He, Luyin Cao, Valentina E. Balas, Pamela McCauley, Fuqian Shi, Curvature manipulation of the spectrum of Valence-Arousal-related fMRI dataset using Gaussian-shaped Fast Fourier Transform and its application to fuzzy KANSEI adjectives modeling, Neurocomputing, vol. 174, pp.1049-1059, 2016
[41] Zeeuw, P.M. (1998), "Wavelet and image fusion," CWI, Amsterdam, March 1998
[42] Abdul Hadi Abdul Razak, Aladin Zayegh, Rezaul K. Begg and Yufridin Wahab, Foot Plantar Pressure Measurement System: A Review, Sensors vol. 12, no.7, pp.9884-9912, 2012.
[43] S. Zheng, K. Huang, T. Tan, D. Tao, A cascade fusion scheme for gait and cumulative plantar pressure image recognition, Pattern Recognition, vol. 45, no.10, pp.3603-3610, 2012.
[44] S. Basu, H. Zhuang, A. Alavi, FDG PET and PET/CT imaging in complicated diabetic plantar, PET Clinics, in special issue: PET Imaging of Infection and Inflammation.vol. 7, no.2,pp. 151-160, 2012.
[45] N. Dey, A.P. Roy, M. Pal, A. Das, FCM based blood vessel segmentation method for retinal images, International Journal of Computer Science and Network (IJCSN), vol. 1, no. 3, 2012.
[46] Ahmed S. S., Dey, N., Ashour A.S., et al., Effect of fuzzy partitioning in Crohn's disease classification: a neuro-fuzzy-based approach, Med Biol Eng Comput (2016). Doi: 10.1007/s11517-016-1508-7
[47] S. Hore, S. Chakroborty, A.S. Ashour, N. Dey, D. Sifaki-Pistolla, T. Bhattacharya, S.R. Chaudhuri, Finding Contours of Hippocampus Brain Cell Using Microscopic Image Analysis. Journal of Advanced Microscopy Research, vol. 10, no. 2, pp.93-103, 2015.

Dan Wang is a Ph.D student in Tianjin Key Laboratory of Process Measurement and Control, School of Electrical Engineering and Automation, Tianjin University, P.R. China, and she also is a joint assistant professor in Wenzhou Vocational College. She holds master degree in computer science and technology and her research interest include multi-sensor data fusion, medical sensor imaging, and data mining.

Zairan Li is currently a Ph.D student in Tianjin Key Laboratory of Process Measurement and Control, School of Electrical Engineering and Automation, Tianjin University, P.R. China, and holds a master degree in control system and application in Huazhong University of Science and Technology, P.R. China, and Dr. Zairan Li also was an associate professor in artificial design at Wenzhou Vocational College. His research interest includes fuzzy inference system, artificial intelligence, control system and multi-sensor data fusion.

Luying Cao is a master student at College of Information and Engineering, Wenzhou Medical University, China; her research interests include biomechanical engineering, artificial intelligence in bio-techniques, BP neuro-network, and data fusion for foot pressure distribution research.

Valentina E. Balas is currently Full Professor in the Department of Automatics and Applied Software at the Faculty of Engineering, "AurelVlaicu" University of Arad, Romania. She holds a Ph.D. in Applied Electronics and Telecommunications from Polytechnic University of Timisoara. Dr. Balas is author of more than 190 research papers in refereed journals and International Conferences. Her research interests are in Intelligent Systems, Fuzzy Control, Soft Computing, Smart Sensors, Information Fusion, Modeling and Simulation. She is the Editor-in Chief to International Journal of Advanced Intelligence Paradigms (IJAIP) and to International Journal of Computational Systems Engineering (IJCSysE), member in Editorial Board member of several national and international journals and is evaluator expert for national and international projects. She was the General Chair of the International Workshop Soft Computing and Applications 2005-2016 held in Romania and Hungary. Dr. Balas participated in many international conferences as Organizer, Session Chair and member in International Program Committee. She is a member of EUSFLAT, ACM and a Senior Member IEEE, member in TC – Fuzzy Systems (IEEE CIS), member in TC - Emergent Technologies (IEEE CIS), member in TC – Soft Computing (IEEE SMCS). Dr. Balas was Vice-president (Awards) of IFSA International Fuzzy Systems Association Council (2013-2015) and is a Join Secretary of Joint Secretary of the Governing Council of Forum for Interdisciplinary Mathematics (FIM), - A Multidisciplinary Academic Body, India.

NilanjanDey, PhD., is an Asst. Professor in the Department of Information Technology in Techno India College of Technology, Rajarhat, Kolkata, India. He holds an honorary position of Visiting Scientist at Global Biomedical Technologies Inc., CA, USA and Research Scientist of Laboratory of Applied Mathematical Modeling in Human Physiology, Territorial Organization Of- Sgientifig and Engineering Unions, BULGARIA, Associate Researcher of Laboratoire RIADI, University of Manouba, TUNISIA. He is the Editor-in-Chief of International Journal of Ambient Computing and Intelligence (IGI Global), US, International Journal of Rough Sets and Data Analysis (IGI Global), US, and the International Journal of Synthetic Emotions (IJSE), IGI Global, US. He is Series Editor of Advances in Geospatial Technologies (AGT) Book Series, (IGI Global), US, Executive Editor of International Journal of Image Mining (IJIM), Inderscience, Regional Editor-Asia of International Journal of Intelligent Engineering Informatics

This article has been accepted for publication in a future issue of this journal, but has not been fully edited. Content may change prior to final publication. Citation information: DOI 10.1109/JSEN.2016.2641501, IEEE Sensors Journal

(IJIEI), Inderscience and Associated Editor of International Journal of Service Science, Management, Engineering, and Technology, IGI Global. His research interests include: Medical Imaging, Soft computing, Data mining, Machine learning, Rough set, Mathematical Modeling and Computer Simulation, Modeling of Biomedical Systems, Robotics and Systems, Information Hiding, Security, Computer Aided Diagnosis, Atherosclerosis. He has 10 books and 180 international conferences and journal papers. He is a life member of IE, UACEE, ISOC etc. https://sites.google.com/site/nilanjandeyprofile/

Amira S. Ashour,PhD.,is an Assistant Professor and Vice Chair of Computer Engineering Department, Computers and Information Technology College, Taif University, KSA. She has been the vice chair of CS department, CIT college, Taif University, KSA for 5 years. She is in the Electronics and Electrical Communications Engineering, Faculty of Engineering, Tanta University, Egypt. She received her PhD in the Smart Antenna (2005) from the Electronics and Electrical Communications Engineering, Tanta University, Egypt. Her research interests include: image processing, Medical imaging, Machine learning, Biomedical Systems, Pattern recognition, Signal/image/video processing, Image analysis, Computer vision, and Optimization. She has 4 books and about 60 published journal papers.She is an Editor-in-Chief for the International Journal of Synthetic Emotions (IJSE), IGI Global, US. She is an Associate Editor for the IJRSDA, IGI Global, US as well as the IJACI, IGI Global, US. She is an Editorial Board Memberof the International Journal of Image Mining (IJIM), Inderscience.

Pamela McCauley is a nationally recognized speaker, entrepreneur, author and full professor in the Department of Industrial Engineering and Management Systems at the University of Central Florida where she leads the Human Factors in Disaster Management Research Team. She previously held the position of Martin Luther King, Jr. Visiting Associate Professor of Aeronautics and Astronautics at the Massachusetts Institute of Technology (MIT). She is the author of over 80 technical papers, book chapters and conference proceedings. In 2012, Dr. McCauley authored; Transforming Your STEM Career Through Leadership and Innovation: Inspiration and Strategies for Women, a practical research-based approach on the growing need for leadership and innovation in America, particularly among women and STEM professionals.

Sifaki-Pistolla Dimitra is an epidemiology researcher and GIS expert in the Clinic of Social and Family Medicine, Faculty of Medicine, University of Crete. She holds a Master degree in Public health and epidemiology and is a PhD candidate of cancer epidemiology. She currently works as a project manager and a geospatial analyst in the regional Cancer Registry of Crete, Greece. She is also a research associate in the clinics of Clinical Bacteriology – Parasitology - Zoonoses, Gastroenterology, Pulmanology and Oncology in the University hospital of Crete. She has a four years educational experience in the pre-graduate program of the Faculty of Medicine and the MPH program of the same department (subjects: epidemiology, analytics, spatial epidemiology and GIS in medicine). She is a member of the Greek team of EDENext (Biology and control of vector-borne infections in Europe) and has working experience from several European (FP7) or national funded projects in health research. Her research interests include: public health, epidemiology, wellbeing, spatio-temporal statistics, Geographical Information Systems (GIS), data mining, mathematical modeling and algorithms, prediction models, interpolation techniques, time-series models, quantitative and qualitative analysis, analysis of biology systems, 2D and 3D spatial modeling, methodological design. She currently has 36 published papers and a special issue in the Science PG, she has participated in a range of conferences, while she was a member of the organizing committee of one European and one local conference.

Fuqian Shi (M'08-SM'10) was graduated from College of Computer Science and Technology, Zhejiang University and got his PhD on Engineering, now he is an associate professor at College of Information and Engineering, Wenzhou Medical University, and also as a visiting associate professor at Department of Industrial Engineering and Management System, University of Central Florida, USA from 2012 to 2014. He is a senior member of IEEE, Membership of ACM, and sever as over 20 committee board membership of international conferences, his research interests include fuzzy inference system, artificial neuro networks, and biomechanical engineering; Dr. Shi also serve as associate editors of International Journal of Ambient Computing and Intelligence (IJACI), International Journal of Rough Sets and Data Analysis (IJRSDA), and special issue editor of fuzzy engineering and intelligent transportation in INFORMATION: An International Interdisciplinary Journal. He published over 40 journal papers and conference proceedings.